

**UV-LIGHT ASSISTED PHOTODEGRADATION AND ANTIBACTERIAL ACTIVITY OF
ACTIVATED CHARCOAL SUPPORTED CADMIUM DOPED ZnO
NANOCOMPOSITE MATERIAL**

S. Prabha, V.L. Chandraboss, J.Kamalakaran and *S. Senthilvelan

Department of chemistry, Annamalai University, Annamalai Nagar 608002, India

Article History: Received 15th December,2014, Accepted January 30th 2015, Published 31st January,2015

ABSTRACT

In the present work, ZnO, Cd/ZnO and AC-Cd/ZnO nanoclusters were prepared using precipitation method. The synthesized samples were characterized using X-ray powder diffraction (XRD) high resolution scanning electron micrographs (HR-SEM) with energy dispersive X-ray analysis (EDX), photoluminescence (PL) UV-Vis diffuse reflectance spectroscopy (DRS) and Fourier transform Raman analysis (FT-RAMAN). The XRD and SEM studies reveal that the synthesized ZnO nano materials have hexagonal wurzite structure with average crystalline size ~28 nm. Photocatalytic activity under ultra violet (UV) light exposure has been studied using methylene blue (MB) dye as test contaminant. A possible mechanism is proposed to explain the charge carrier recombination and interfacial charge transfer processes. It has been found the optimum amount of Cd²⁺ doping and increased adsorption ability of light due to high separation rate of photoinduced charge carriers, which play an important role enhancing the overall photocatalytic performance significantly. Further its antibacterial activity against two gram positive and two gram negative bacterial strain is studied

Keywords: Nanocomposites, Photocatalytic Activity UV irradiation, Raman Spectroscopy, X-Ray diffraction, Antibacterial activity.

1.INDRODUCTION

Clean unadulterated water does not occur in the environment. Water contamination is a any undesirable alter in the state of water, contaminated with destructive substances. It is the second mainly vital environmental concern next to air pollution (Ramandeep Singh Gambhir et al, 2012) Dyes are normally used in the many industries including printing process, textile, plastic, cosmetics and the overload dyes are released into the effluent stream as waste after colouring the fabric. Most of the unspent dyes produces undesirable effluents and usually discharged without treatment (Susheela Bai Gajbhiye, 2012). These adversely affect the quality of water, inhibit sunlight penetration and reduce photosynthetic reactions. In addition, some dyes are either toxic or carcinogenic. Currently available water treatment technologies either concentrate the pollutants present by transferring them to other phases (adsorption or coagulation) or involve high operating costs with possible generation of toxic secondary pollutants into the ecosystem (Abi et al, 2013). Using nanometer semiconductor photocatalysts, such as ZnO, CdS, TiO₂, and SnO₂, to purify environment is exactly emphasized. As one of the most important semiconductor photocatalysts, zinc oxide (ZnO) has

stimulated great research interest due to its unique physical and chemical properties, such as cheap, harmless, high photosensitivity and stability (Yin et al, 2000; Lee et al, 2001). ZnO is a semiconductor with a wide band gap (3.3 eV) and a large exciton binding energy and is abundant in nature and environmentally friendly; these characteristics make this material attractive for many applications, including solar cells, optical coatings, photocatalysts, and electrical devices (Nirmala et al, 2011). Researches have shown that ZnO exhibits better photocatalytic efficiency than TiO₂ for the removal of organic compounds in water matrices (Wei Liu et al, 2013). It is the most important material to eliminate organic pollutants in waste water such as reactive brilliant red K-2BP (Liu et al, 2012), methylene blue (Sun et al, 2009), Acridine orange (Khan et al, 2011), rhodamine B (Li et al, 2012), methyl orange (Xu et al, 2012), and polyvinyl alcohol in aqueous solutions (Lin et al, 2013). Sun et al. reported that dumbbell-shaped ZnO photocatalyst showed a 99.6% decolorization efficiency of MB within 75 min under UV light (365 nm) which is higher than the commercial ZnO performance. Various conventional techniques or methods such as co-precipitation, sol-gel method, impregnation method, hydrothermal method etc. are used for synthesizing nanoparticles as well as synthesis of metal doped nanoparticles (Zhang et al, 2007). Recently, these methods are found to be more efficient for doping of metal ions for improving the photocatalytic efficiency of catalysts by

*Corresponding author: Dr. S. Senthilvelan, Department of chemistry, Annamalai University, Annamalai Nagar 608002, India

decreasing the band gap which in turn increases the absorption of photons in the visible region of the light (Samadi et al, 2012). Among various dopants, currently the doping of Cd in ZnO has received a great attention as by doping ZnO with Cd, its absorption edge can be red-shifted (Karunakaran et al, 2012). In addition to this, due to almost similar ionic radius of Zn^{2+} (0.60 Å) and Cd^{2+} (0.74 Å), the synthesized materials can retain the stable wurtzite hexagonal phase of ZnO. There are very rare reports to use Cd-doped ZnO nanomaterials as a photocatalyst for photocatalytic degradation of organic dyes (Wu et al, 2011). In a recent report, Karunakaran et al. have demonstrated the use of nanocrystalline Cd-doped ZnO for the photocatalytic degradation of Rhodamine B. Many researchers have been attempting to modify the catalyst surface to increase the efficiency of these processes. To increase the adsorption capacity of organic compounds, researchers have explored supporting ZnO on such porous materials as silicon dioxide (SiO_2) (Dinget al., 2000), zirconium oxide (ZrO_2) (Chen et al., 2001; Masanori et al., 2002), quartz (Herrmann et al., 1997), zeolites, activated carbon (AC) (Matos et al., 1998; Tsumura et al., 2002; Sobana et al., 2008). In particular, activated carbon (AC) has been extensively researched as a support for heterogeneous catalysis (Subramani et al, 2007).

2. EXPERIMENTAL SECTION

Chemicals

Cadmium acetate dihydrate, Zinc acetate dihydrate, activated charcoal, hydrochloric acid, ethanol and methylene blue were the guaranteed reagents of sigma Aldrich and are used as such. Deionized water was used for all the reactions and treatment processes. All glasswares were cleaned with chromic acid followed by thoroughly washing with distilled water. Chemical structure of methylene blue is shown in Fig. 1

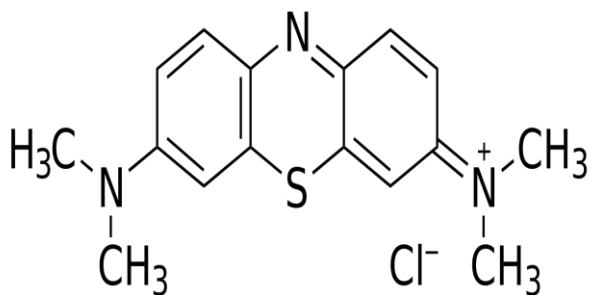


Figure 1: Chemical structure of Methylene Blue

SYNTHESIS OF AC-SUPPORTED Cd- DOPED ZnO NANO COMPOSITE MATERIALS

AC-Supported Cd doped ZnO nanocomposite material was synthesized by precipitation method. Initially cadmium acetate dihydrate (0.2 M) and Activated charcoal were dissolved in anhydrous ethanol (solution A). 0.8 ml of Zinc acetate dihydrate dissolved in ethanol is taken as another solution B. The solution B is added to Solution A and stirred well. To this 2 NaOH pellets dissolved in water is added at room temperature under vigorous stirring until the precipitate formed. The obtained precipitate was washed with water and ethanol. Then the precipitate was collected and dried in oven

at 100°C for 12 hrs. The resulting powder was finally calcinated at 300°C at 2 hrs.

PHOTOCATALYTIC ACTIVITY

The photocatalytic activity of the prepared photocatalysts was evaluated by the photodegradation of MB by using multilamp photoreactor. The light source was a UV lamp (365nm). The reaction was maintained at ambient temperature (303 K). In a typical experiment, aqueous suspensions of dye (50 mL, 1×10^{-4} mol L⁻¹) and 0.08 g of the photocatalyst were loaded in the reaction tube. Prior to irradiation, the suspension was magnetically stirred in the dark to ensure the establishment of an adsorption/desorption equilibrium. The suspension was kept under constant air-equilibrated condition. At the intervals of given irradiation time. The reaction solution was measured spectrophotometrically (660 nm) by diluting it five times to keep the absorptions within the Beer-Lambert law limit.

ANTIBACTERIAL ACTIVITY STUDY

Antibacterial activities of the synthesized ZnO, Cd/ZnO and AC-Cd/ZnO nanomaterials were determined in comparison with Ciprofloxacin, using the disc diffusion assay method [Seely, 1975; Barry, 1976], is a means of measuring the effect of an antimicrobial agent against bacteria grown in culture. The bacteria in question are swabbed uniformly across a culture plate. A filter-paper disk, impregnated with the compound to be tested, is then placed on the surface of the agar. The compound diffuses from the filter paper into the agar. The concentration of the compound will be highest next to the disk, and will decrease as distance from the disk increases. If the compound is effective against bacteria at a certain concentration, no colonies will grow where the concentration in the agar is greater than or equal to the effective concentration. This is the zone of inhibition. Thus, the size of the zone of inhibition is a measure of the compound's effectiveness: the larger the clear area around the filter disk, the more effective the compound. Approximately (20 mL) of molten and cooled media (Nutrient agar) was poured in sterilized Petri dishes. The plates were left overnight at room temperature to check for any contamination to appear. The bacterial test organisms were grown in nutrient broth for 24 h. A (100 mL) nutrient broth culture of each bacterial organism (1×10^8 cfu/mL) was used to prepare bacterial lawns (cfu=number of colony forming unite). Antibiotic disks of 5 mm in diameter were impregnated with ZnO, Cd/ZnO and AC-Cd/ZnO nanomaterials solution (60 µg/ml). The plates were incubated at 37°C and were examined for evidence of zones of inhibition, which appeared as a clear area around the wells. The diameter of such zones of inhibition was measured using a meter ruler and the mean value for each organism was recorded and expressed in millimeter.

ANALYTICAL METHODS

High resolution Scanning Electron Microscopy (HR-SEM) and Elementary Dispersive X-ray (EDX) analysis experiments were carried out on a FEI Quanta FEG 200 instrument with EDX analyzer facility at 25 kV. XRD spectra was recorded on the X'PERT PRO model X-ray diffractometer from Pan Analytical instruments operated at a voltage of 40 kV and a current of 30 mA with Cu K α

radiation. FT-RAMAN spectra were recorded with an integral microscope Raman system RFS27 spectrometer equipped with 1024 - 256 pixels liquefied nitrogen-cooled germanium detector. The 1064 nm line of the Nd:YAG laser (red laser) was used to excite. To avoid intensive heating of the sample, the laser power at the sample was not higher than 15 mW. Each spectrum was recorded with an acquisition time of 18 s. UV-vis (ultraviolet and visible light) absorbance spectra were measured over a range of 200–800 nm with a Shimadzu UV-1650PC recording spectrometer using a quartz cell with 10 mm of optical path length. Photoluminescence spectra at room temperature were recorded using a perkin-Elmer LS 55 fluorescence spectrometer. Nano particles were dispersed in chloroform and excited using light of wavelength 300nm. The nanoparticles size and structure confirmations were done by Transmission Electron Microscopy (TEM) using PHILIPS CM200

3.RESULT AND DISCUSSION

HR-SEM MICROGRAPH ANALYSIS

Figure (2a), (2b) and (2c) shows the HR-SEM images of the as prepared ZnO, Cd/ZnO and AC-Cd/ZnO. The surface morphology of ZnO, Cd/ZnO and AC-Cd/ZnO has been studied using High Resolution Scanning Electron Micrographs. The SEM investigations revealed that the synthesized particles were of nanometer size in all of the samples. ZnO image indicates that the highly dispersed nano materials have been obtained with an average diameter of ~20 nm. The Cd doped ZnO exhibits hexagonal shaped nanoparticles and are highly aggregated such agglomeration makes it difficult to evaluate the grain size from SEM images and average diameter was calculated as ~45 nm. In the case of AC-Cd/ZnO, shows that the hexagonal shaped nano materials grown in high density. The average diameter of the grown nanomaterials was about ~50±10 nm.

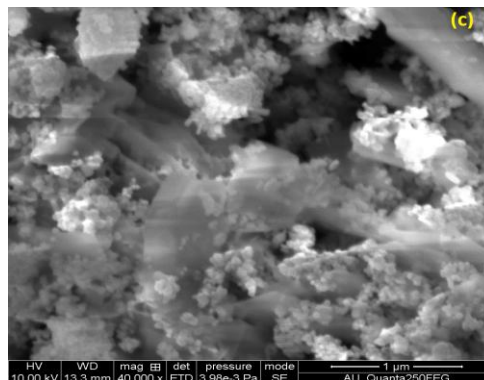
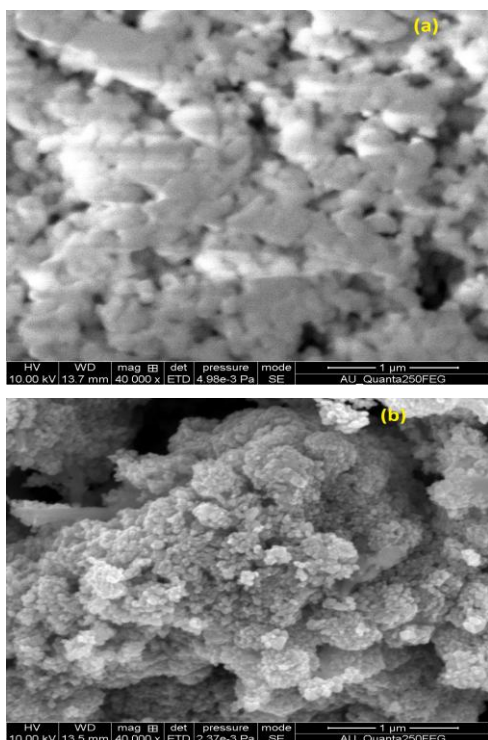


Figure 2: HR-SEM images of (a) ZnO (b) Cd/ ZnO (c) AC-Cd/ ZnO

The observation particle size of the Cd/ZnO nanomaterials was greater than that of AC-Cd/ZnO nanomaterials and this size decrease can be correlated with the observed increase of the surface area (Mohd Athar, 2014). Decrease the nanometer size of the particles led to an increased surface area and a consequent increase in the number of photocatalytic reaction sites, properties that improved the photocatalytic activity (Kai-sheng Yu et al, 2013).

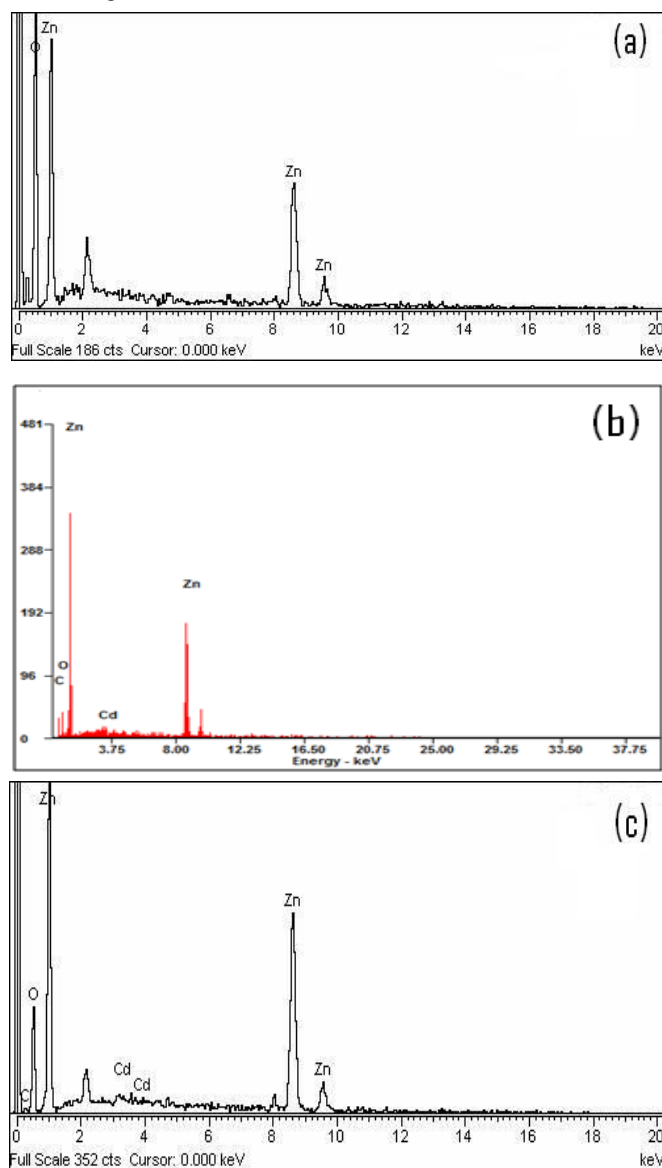


Figure :3 (a) EDX Spectrum of ZnO (b) Cd/ZnO (c) AC-Cd/ZnO

Figure 3(a), 3(b) and 3(c) shows the EDX images of the as prepared ZnO, Cd/ZnO and AC-Cd/ZnO. EDX spectrum is used to analyze the elemental composition of the hybrid particles. EDX analysis confirms only Zinc, cadmium and oxygen present Cd/ZnO (Figure 3b), where as Zinc, cadmium, oxygen and carbon present in AC-Cd/ZnO composite material (Figure 3c). EDX analysis of the composite sample confirms a doping of the Cd and C in the ZnO material.

POWDER XRD

The obtained XRD of the ZnO, Cd/ZnO and AC-Cd/ZnO nanomaterial are shown in Fig. 4A, 4B and 4C. It is seen from figure 1(A) that peaks appear at 31.87° , 34.53° , 36.25° , 47.20° , 56.82° and 63.18° . The diffractogram of the sample reveals that all the peaks are in good agreement with the JCPDS data belonging to hexagonal ZnO structure (Card No. 36-1451). The corresponding reflecting planes are (100), (002), (101), (102), (103) and (110), respectively. The (101) peak appears with a maximum intensity at 36.25° . The average crystallite size of the samples, evaluated by the Scherrer formula (Cullity B D. 1978), is about 13 nm. Interestingly, figure 4B shown no diffraction peak corresponds to Cd ion was detected in the pattern which suggest that Cd^{2+} ions would uniformly substitute the Zn^{2+} ions into the lattices of ZnO which was may be due to almost similar ionic radius of Cd^{2+} (0.74 \AA) and Zn^{2+} (0.60 \AA) ions (Ahmad Umar et al, 2012). With the increasing of the Cd-doped concentration, the intensity of the peaks slightly decreases. There are no other phases to be found in the pattern of XRD. In addition, the broad peak at the 2θ value of 22.80° corresponds to an presence of graphite-like carbon (d (002), JCPDS; 41-1487).

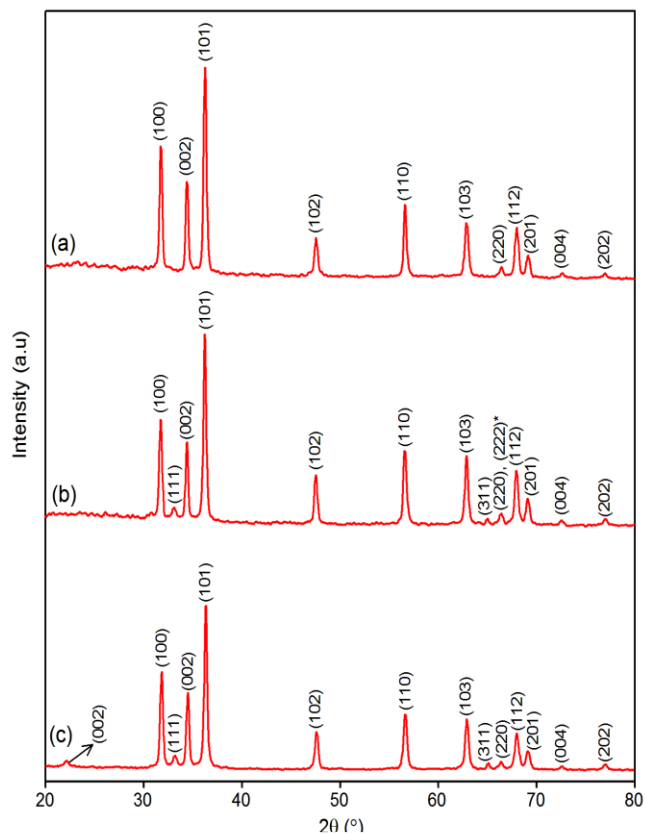


Figure 4: XRD patterns of (A) ZnO Nano material, (B) Cd/ZnO nanocomposite materials and (C) AC-Cd/ZnO Nanocomposite material

RAMAN SPECTRUM

Figure 6a, 6b and 6c shows the Raman spectrum of ZnO, Cd/ZnO and AC-Cd/ZnO nanomaterial. ZnO has a wurtzite crystal structure and belongs to C_{6v} group. According to group theory analysis, the $A_1+E_1+2E_2$ modes are Raman active. A_1 and E_1 modes are polar and split into transverse optical (TO) and longitudinal optical (LO) components. The E_2 (high) mode is characteristic of the wurtzite phase [Lupan et al, 2010]. No differences in the Raman spectra were observed for concentration as low as Cd as compared to pure ZnO. No Raman peaks of cd appeared in the spectrum of the AC-Cd-doped ZnO nanostructures, indicating no secondary phase in copper-doped samples, which is consistent with the XRD results. The intense peak near 439 cm^{-1} due to the E_2 (high) mode displays a clear asymmetry towards low frequencies. ZnO spectrum the peak at 381.6 cm^{-1} corresponds to $A_1(\text{TO})$, 412 cm^{-1} corresponds to $E_1(\text{TO})$. The peak at 580 cm^{-1} is positioned between $A_1(\text{LO})$ and $E_1(\text{LO})$. The high intensity of the 1362 cm^{-1} and 1695 cm^{-1} , attributed to the D- and G-bands of Carbon, respectively.

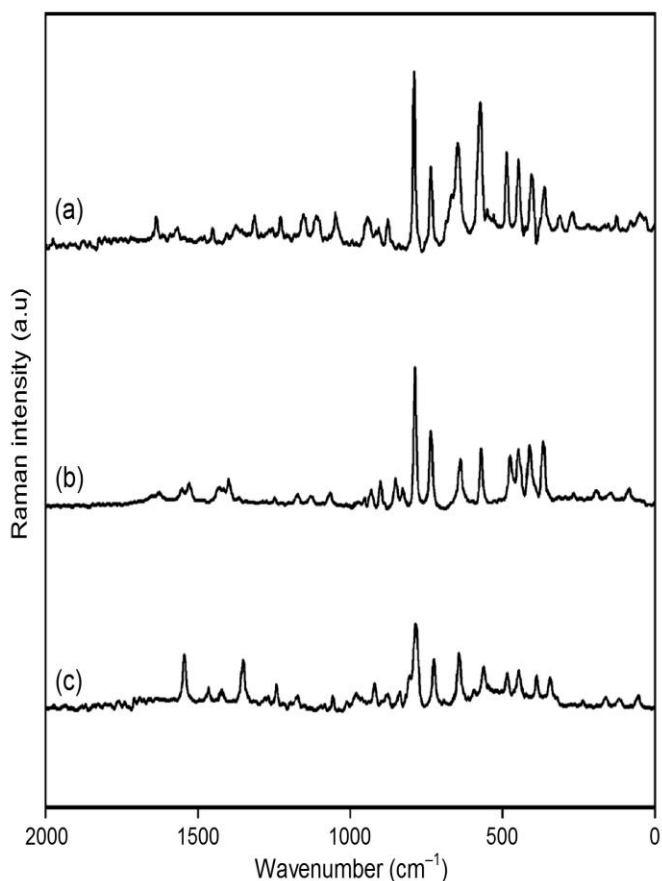


Figure 5: FT-RAMAN Spectra of (a) Cd/ZnO nanocomposites (b) Cd/ZnO nanomaterials and (c) AC-Cd/ZnO nano composite material

PL SPECTRA

Photoluminescence spectra of ZnO, Cd/ZnO and AC-Cd/ZnO are shown in figure 5a,5b and 5c respectively. Photocatalysts generate electrons and holes after being activated by light, and the recombination of some electrons and holes can release energy in the form of fluorescence emission. All of the spectra showed two emission bands located at 392 and 491 nm. While the sharper 392-nm emission band has typically been assigned to the near-band-edge emission in

ZnO, the band in the visible spectral range (showing a peak at 491 nm) has been attributed to the recombination of photogenerated holes with singly ionized charge states of the intrinsic defects such as oxygen vacancies, Zn interstitials, or impurities. The PL Spectrum of Cd/ZnO and AC-Cd/ZnO nanoComposites show as in the case of undoped ZnO and there is no significant shift in the position of the undoped ZnO. AC-Cd/TiO₂ gave four emissions at 360, 410, 493 and 510 nm. It is also observed that the samples exhibits low resistivity after doping, confirms by the blue-green emission intensity decreased when the doping ratio increases (Arun et al, 2013). The intensity of AC-Cd/ ZnO PL emission is less when compared to ZnO and Cd/ ZnO nano composite materials. A weaker PL emission signal is commonly indicative of higher photocatalytic activity (Chen et al, 2008).

UV-VIS DIFFUSE REFLECTANCE SPECTROSCOPY

Figure 7 shows the diffuse-reflectance spectra, as a function of wavelength for samples. The inset of Figure 7 shows the band-gap as a function of the doping concentrations obtained from diffuse reflectance spectra. The band-gap energy of the Cd-doped ZnO samples was calculated from the diffuse-reflectance spectra by plotting the square of the Kubelka-Munk function $F(R)2$ vs. the energy in electron volts. The linear part of the curve was extrapolated to $F(R)2 = 0$ to calculate the direct band-gap energy. It is seen that the absorption edge shifts to lower energies/longer wavelength. The band gap energy calculated from derivative of the spectra is 3.35 eV for ZnO and 3.28 eV for Cd/ZnO and 3.26 eV for AC-Cd/ZnO nanomaterials. The lower value of energy of AC-Cd/ZnO helped in increasing number of electron hole pair thus enhancing the dye degradation.

PHOTOCATALYTIC ACTIVITY

Present measurements report the photocatalytic activity ZnO, Cd/ZnO and AC-Cd/ZnO nanomaterials by degradation of MB dye under UV light exposure. When a photon of UV light strikes the ZnO surface, an electron (e⁻) from its valence band jumps to the conduction band leaving behind a positively charged hole (h⁺) in valance band. The photocatalytic active centres are formed on the surface of ZnO due to increase negative charge in the conduction band. The valence band hole (h⁺) reacts with the chemisorbed H₂O molecules to form reactive species such as .OH radicals, which subsequently react with dye molecules to cause their complete degradation. e⁻ can react with O₂ to produce superoxide radical anion of oxygen(O²⁻) (Mahmoodi et al., 2006). The •OH and O²⁻ produced in the above manner can then react with the dye to form other species and is thus responsible for the discoloration of the dye.

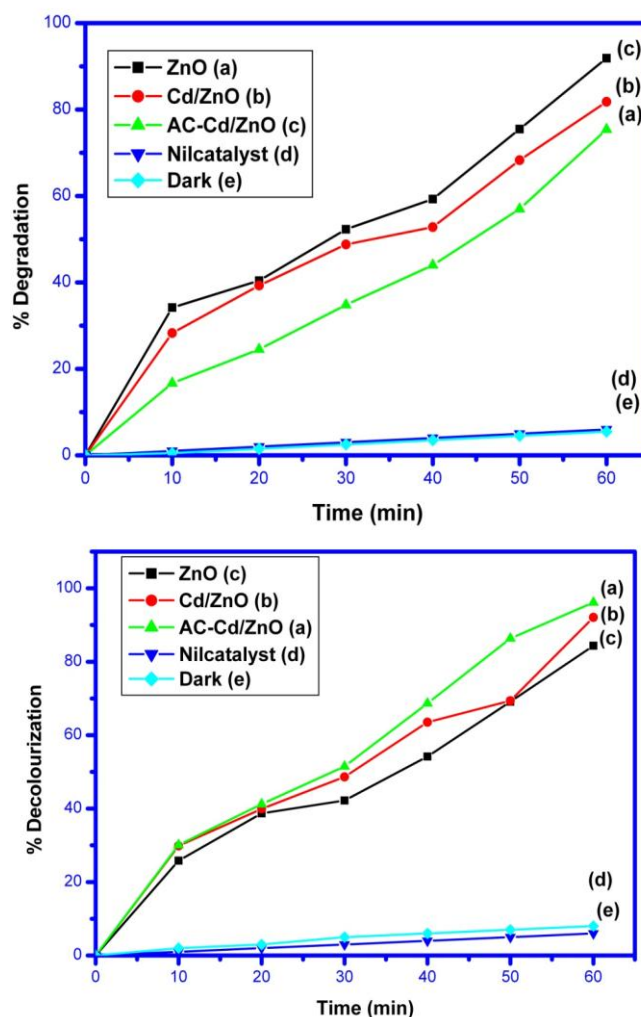


Fig: 8 (a) Photodegradability of Methylene Blue by ZnO (curve c) , Cd/ZnO (curve b) and AC-Cd/ZnO (curve c) (b) Decolourization of methylene blue by ZnO (curve c), Cd/ZnO (curve b) and AC-Cd/ZnO (curve c)

These ions reduce the recombination of h⁺ and e⁻ and favour the formation of .OH radicals. It is proposed that increase in photocatalytic activity with Cd doping can be explained by their ability to trap electrons and generate holes so they act as electron scavengers. The retardation of the electron-hole recombination will increase the photocatalytic efficiency of the ZnO nanocrystals photocatalysts and, consequently,

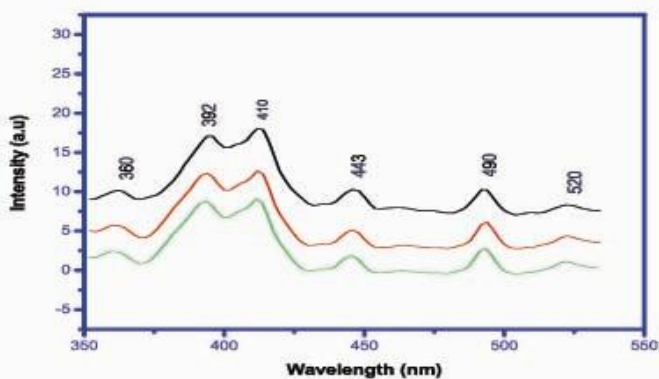


Figure 6: PL Spectra of (a) ZnO (b) Cd/ZnO (c) AC-Cd/ZnO nanomaterials

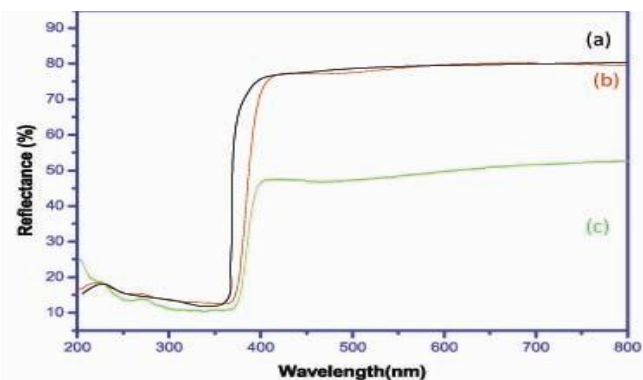


Fig. 7. UV-VIS diffuse reflectance spectroscopy of (a) nanocomposites (b) Cd/ZnO nanoparticles and (c) AC-Cd/ZnO nanocomposite material

accelerate hydroxyl radical formation which will enhance the rate of MB degradation.

The UV-vis absorbance spectrum of MB solution shows absorption peaks at 243, 286 and 664 nm. The characteristic absorption peak at 664 nm was used to track the photocatalytic degradation process. The comparative study of photocatalytic activity of ZnO, Cd/ZnO and AC-Cd/ZnO photocatalysts for photodegradation of MB was shown in figure 8a and 8b. AC-Cd/ZnO exhibited excellent photocatalytic activity for MB under UV light irradiation when compared to that of ZnO and Cd/ZnO.

The effect of time on the degradation of MB was examined under UV light irradiation in the reaction time ranging from 0 to 60 minutes. Samples were withdrawn at different time intervals after photodegradation and centrifuged immediately and percentage mineralisation was studied.

Results show that as time increases the percentage decolorization and degradation increases. The photocatalytic activity of the sample AC-Cd/ZnO is the highest, and the degradation of MB can be nearly up to 91.6% after 1 h of irradiation. It is because that the oxygen vacancies and defects could become capture centers of photo-induced electrons to effectively inhibit the recombination of electrons and holes. However, when the concentration of Cd²⁺ is excess, the oxygen vacancies and defects would become recombination centers (Song et al, 2010; Ji et al, 2010) So the ZnO nanomaterial doped with a small amount of Cd²⁺ could enhance the photocatalytic activity.

ANTIBACTERIAL ACTIVITY

The bactericidal activity of the crude and annealed samples of ZnO, Cd/ZnO and AC-Cd/ZnO nanomaterials were investigated against Gram (+ve) and Gram (-ve) bacteria, as presented in Figure 9 and Table 1. These three samples showed antibacterial activity against all the tested pathogenic organisms. AC Supported Cd doped ZnO sample showed more activity against bacteria than undoped ZnO and Cd doped ZnO sample. Among the various gram positive bacteria used, The AC Supported Cd doped ZnO sample showed maximum activity (zone of inhibition 14mm) against *Bacillus subtilis* whereas, it showed moderate activity against *Pseudomonas aeruginosa* (zone of inhibition 13mm). Pure ZnO sample showed maximum activity against *Streptococcus pyogenes* (zone of inhibition 13mm).

Table 1. Antibacterial activity (Disc diffusion method)

Sl. No	Bateria	Standard antibiotic disc	Zone of inhibition (mm)			
			ZnO	Cd/ZnO	AC-Cd/Zn	Control (DMSO)
1	<i>Bacillus subtilis</i>	20	09	11	14	-
2	<i>Escherichia coli</i>	26	11	12	12	-
3	<i>Pseudomonas aeruginosa</i>	22	11	12	13	-
4	<i>Streptococcus pyogenes</i>	24	13	15	16	-

*ciprofloxacin

Our results explain ZnO and its doped nano materials which act against the water contamination, allergic reactions, food poisoning and also act as drug resistant pneumonia and advantage of using these oxides as antimicrobial agents is that they contain mineral elements essential to human and exhibit strong activity even when administrated in small

amounts. AC-Cd/ZnO showed a high bactericidal efficacy so this material is suggested to incorporate with the lab fabrics, gloves etc. Antimicrobial garments may be useful for individuals coming into contact with patients such as visitors, nurses, doctors and other healthcare workers.

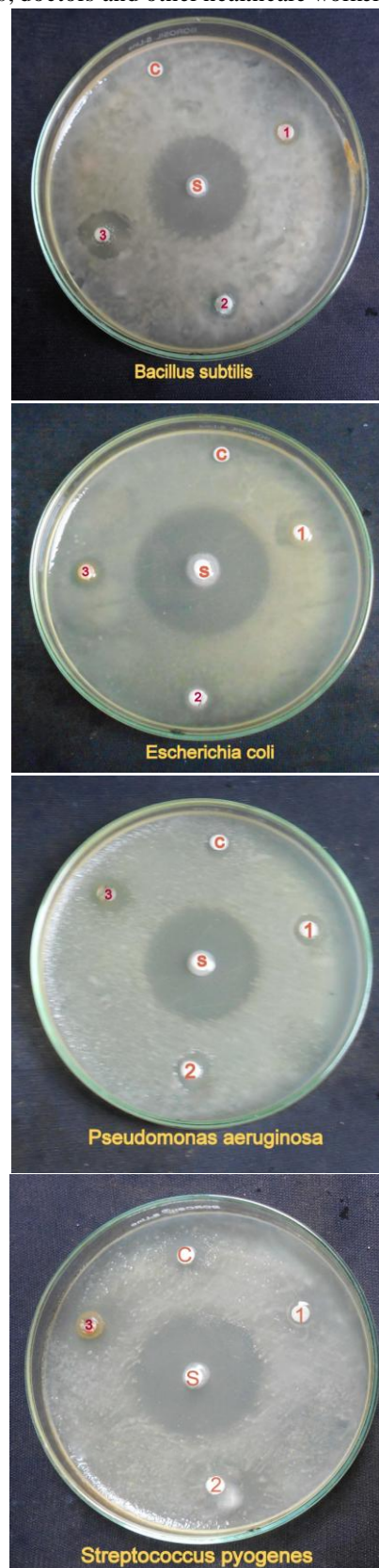


Figure 9. The antibacterial effect of synthesized ZnO, Cd/ZnO and AC-Cd.ZnO nanoparticles; (a) *Bacillus subtilis*, (b) *Escherichia coli*, (c) *Pseudomonas aeruginosa* (d) *Staphylococcus pyogene*

4. CONCLUSION

AC Supported cadmium doped ZnO nanocomposite material was prepared by a precipitation method. This material was characterized by powder X-ray diffraction (XRD), high resolution scanning electron micrographs (HRSEM) with energy dispersive X-ray analysis, photoluminescence (PL) and Fourier transform Raman analysis (FT-RAMAN). These results confirmed the formation of AC-Cd/ZnO nanocomposite material. HR SEM and XRD analysis of ZnO and Cd/ZnO showed the average size of as 12.3nm, AC-Cd/ZnO showed the average particle size of as 5nm. Moreover the decrease in particle size can be correlated with increase of the surface area. The EDX shows the presence of C and Cd in the ZnO material. XRD reveal the all strong peaks can be indexed as Hexagonal wurzite form of ZnO. PL Spectra explain the suppression of recombination of the photogenerated electron hole pairs by AC-Cd/ZnO nano material. AC-Cd/ZnO reveals enhanced photocatalytic activities as compared to ZnO and Cd/ZnO for the photodegradation and decolorization of MB under UV light irradiation for 0 to 60 minutes. The mechanism of photocatalytic effect of AC-Cd/ZnO nano composite material has been discussed.

5. REFERENCES

- Abi M. Tadesse et al. 2013. Synthesis, characterization and photocatalytic activities of Ag-n-codoped ZnO nanoparticles for degradation of methyl red, *Bull. Chem. Soc. Ethiop.* 27(2), 221-232.
- Ahmad Umar et al, 2013. Synthesis and Characterizations of Cd-Doped ZnO Multipods for Environmental Remediation Application, *J. Nanosci. Nanotechnol.* 2012, Vol. 12, No. 11.
- Arun S Menon et al, 2013, Studies on structural and optical properties of ZnO and Mn-doped ZnO nanopowders., *Indian Journal of NanoScience*, 1(2) 16-24.
- Barry., A. L. 1976. *The antimicrobial susceptibility test. Principle and Practice*, Lea and Febiger, Philadelphia, 180.
- Chen, H.R., Shi, J.L., Zhang, W.H., Ruan, M.L., and Yan, D.S. (2001). Incorporation of titanium into the inorganic wall of ordered porous zirconium oxide via direct synthesis. *Chem. Mater.* 13, 1035.
- Chen, X.F., Wang, X.C., Hou, Y.D., Huang, J.H., Wu, L., Fu, X.Z., 2008. *J. Catal.* 255(1), 59–67.
- Cullity B D. 1978. *Elements of X-ray diffraction* (M A: Addison-Wesley) 102.
- Ding, Z., Lu, G.Q. and Greenfield, P.F. 2000. A kinetic study on photocatalytic oxidation of phenol in water by silica dispersed titania nanoparticles. *J. Colloid Interf. Sci.* 232, 1.
- F.Xu, J.Chen, L.Guo, S. Lei, and Ni, Y. 2012. "In situ electrochemically etching-derived ZnO nanotube arrays for highly efficient and facilely recyclable photocatalyst," *Applied Surface Science*, vol.258, pp. 8160–8165.
- Herrmann, J.M., Tahiri, H., Ait-ichou, Y., Lassaletta, G., Gonza lez-Elipe, A.R., and Fernandez, A. 1997. Characterization and photocatalytic activity in aqueous medium of TiO₂ and Ag-TiO₂ coatings on quartz. *Appl. Catal. B-Environ.* 139, 219.
- Ji, L.F et al., 2010. Synthesis of Gd-Cd Co-Doped Nano TiO₂ Photocatalyst and Its Photocatalytic Activity[J]. *Journal of Yanan University.* 29:71-75.
- Kai-sheng Yu et al, 2013. Synthesis, Characterization, and Photocatalysis of ZnO and Er-Doped ZnO, *Hindawi Publishing Corporation Journal of Nanomaterials.* 372951, 5.
- Karunakaran, C., Vijayabalan, A. and Manikandan, G. 2012. Photocatalytic and bactericidal activities of hydrothermally synthesized nanocrystalline Cd-doped ZnO Superlattices and Microstruct. 51, 443.
- Khan, S. B., Faisal, M., Rahman, M. M. and Jamal, A. 2011. "Low temperature growth of ZnO nanoparticles: photocatalyst and acetone sensor," *Talanta*, vol. 85, no. 2, pp. 943–949, 2011.
- Lee G H et al., 2001. Blue shift in room temperature photoluminescence from photo-chemical vapor deposited ZnO films[J]. *Thin Solid Films*, 386:117-120.
- Li, J., Lu, G., Wang, Y., Guo, Y. and Guo, Y. 2012. "A high activity photocatalyst of hierarchical 3D flowerlike ZnO microspheres: synthesis, characterization and catalytic activity," *Journal of Colloid and Interface Science*, vol. 377, pp. 191–196.
- Lin, C. C. and Hsu, L. J. 2013. "Removal of polyvinyl alcohol from aqueous solutions using P-25 TiO₂ and ZnO photocatalysts: a comparative study," *Powder Technology*, vol. 246, pp. 351–355.
- Liu, Y., Lv, H., Li, S., Xing, X. and Xi, G. 2012. "Preparation and photocatalytic property of hexagonal cylinder-like bipods ZnO microcrystal photocatalyst," *Dyes and Pigments*, vol. 95, Article ID 443-449.
- Mahmoodi, N.M., Arami, M., Limaee, N.Y., Tabrizi, N.S. 2006. Kinetics of heterogeneous photocatalytic degradation of reactive dyes in an immobilized TiO₂ photocatalytic reactor, *Journal of Colloid and Interface Science* 295, 159–164.
- Masanori, H., Chiaki, N., Keisuke, O., and Michio I. 2002. Direct formation of zirconia-doped titania with stable anatase-type structure by thermal hydrolysis. *J. Am. Ceram. Soc.* 85, 1333.
- Matos, J., Laine, J., and Herrmann, J.M. 1998. Synergy effect in the photocatalytic degradation of phenol on a suspended mixture of titania and activated carbon, *Appl. Catal. B-Environ.* 18, 281.
- Mohd Athar., 2014. *Adv. Mater. Rev.* 1(1), 25-37
- Nirmala, M. and Anukaliani, A. 2011. "Synthesis and characterization of undoped and TM (Co, Mn) doped ZnO nanoparticles," *Materials Letters*, vol. 65, no. 17-18, pp. 2645–2648.
- Ramandeep Singh Gambhir., Vinod Kapoor., Ashutosh Nirola., Raman Sohi and Vikram Bansal. 2012. Water Pollution: Impact of Pollutants and New Promising Techniques in Purification Process, Department of Public Health Dentistry, Department of Oral and Maxillofacial Surgery, Gian Sagar Dental College and Hospital, Rajpura, India, *J Hum Ecol.*, 37(2), 103-109.
- Samadi, M., Asghari Shivaee, H., Zanetti, M., Pourjavadi, A., Moshfegh, A. 2012. Visible light photocatalytic activity of novel MWCNT-doped ZnO electrospun nanofibers, *J. Molecul.*
- Seely H.W. and Van Demark., P. J. 1975. *A Laboratory Manual of Microbiology*, Taraporewala Sons and Co., Mumbai, 55.

- Sobana, N., Muruganandam, M., and Swaminathan, M. 2008. Characterization of AC-ZnO catalyst and its photocatalytic activity on 4-acetylphenol degradation. *Catal. Commun.* 9, 262.
- Song, X.C et al.,2010. Photocatalytic activities of Cd-doped ZnWO₄ nanorods prepared by a hydrothermal process[J]. *Journal of Hazardous Materials*, 179:1122-1127. 220.
- Subramani, A., Byrappa, K., Ananda, S., Lokanatha Rai, K, Lokanatha Rai, K, and Yoshimura M. 2007. Photocatalytic degradation of indigo carmine dye using TiO₂ impregnated activated carbon. *Bull Mater Sci*,30(1):37–41.
- Sun, J.H., Dong, S.Y. , Wang, Y.K. and. Sun, S.P. “Preparation and photocatalytic property of a novel dumbbell-shaped ZnO microcrystal photocatalyst,” *Journal of Hazardous Materials*, vol. 172, no. 2-3, pp. 1520–1526.
- Susheela Bai Gajbhiye.2012. Photocatalytic Degradation Study of Methylene Blue Solutions and Its Application to Dye Industry Effluent, Department of Engineering Chemistry, College of Engineering, Andhra University, Visakhapatnam, 530 003, India, *International Journal of Modern Engineering Research (IJMER)*, 2, 1204-1208.
- Tsumura, T., Kojitani, N., Umemura, H., Toyoda, M., and Inagaki, M. 2002. Composites between photoactive anatase-type TiO₂ and adsorptive carbon. *Appl. Surf. Sci.* 196, 429.
- Wei Liu et al.,2013. Synthesis, Characterization, and Photocatalysis of ZnO and Er-Doped ZnO *Journal of Nanomaterials*, 2,5
- Wu ,J. and Xue, D.2011.Progress of Science and Technology of ZnO as Advanced Material *Sci. Adv. Mater.* 3, 127.
- Yin J et al., 2000.The epitaxial growth of wurtzite ZnO films on LiNbO₃ (0001) substrates[J]. *Journal of Crystal Growth*, 220:281-285.
- Zhang, H.W., Wei, Z.R., Li, Z.Q., Dong, G.Y.2007. Room-temperature ferromagnetism in Fe-doped, Fe- and Cu-codoped ZnO diluted magnetic semiconductor, *Mater. Lett.* 61,3605–3607
